

Electrically Controlled Liquid Crystal Phase Grating for Terahertz Waves

Chia-Jen Lin, Chuan-Hsien Lin, Yu-Tai Li, Ru-Pin Pan, and Ci-Ling Pan, *Senior Member, IEEE*

Abstract—This work demonstrates the feasibility of electrically controlled liquid-crystal-based phase grating for manipulating the terahertz (THz) waves. This device can be utilized as a THz beam splitter and the beam splitting ratio of the zeroth- to the first-order diffractions can be tuned from 10 : 1 to 1 : 1.

Index Terms—Liquid crystal devices, phase grating, submillimeter wave, terahertz (THz) radiation, tunable circuits and devices, ultrafast optics.

I. INTRODUCTION

QUASI-OPTICAL components for submillimeter or terahertz (THz) waves are in high demand due to the recent rapid progress in THz science and technology [1], [2]. For control of properties of electromagnetic waves at all wavelengths, periodic structures such as gratings were widely used for applications such as couplers and filters [3], [4]. The potential for gratings with liquid-crystal-enabled functionalities was also recognized two decades ago [5]. Of late, various tunable THz devices employing nematic liquid crystals (NLCs), such as phase shifters, filters, and switches that are controlled either electrically or magnetically, were demonstrated [6]–[12]. By changing the effective refractive index of the NLC [13], we recently demonstrated a magnetically controlled phase grating for manipulating THz waves [14]. Nonetheless, electrically controlled phase gratings are deemed desirable for many applications. In this work, we propose and demonstrate an electrically controlled phase grating using NLC for THz waves. Performance of the device is in good agreement with theoretical predictions.

II. OPERATION PRINCIPLES AND EXPERIMENTAL SETUPS

The present device is designed as a binary phase grating. It contains alternate sections of two materials with different refractive indices. The electric fields of electromagnetic waves that pass through these two materials, E_1 and E_2 , and the total

Manuscript received December 15, 2008; revised February 26, 2009. First published March 27, 2009; current version published May 15, 2009. This work was supported in part by the National Science Council (NSC) through various grants including NSC 96-2221-E-009-131-MY3, PPAEU-II, and by the ATU program of the Ministry of Education, Taiwan, Republic of China.

C.-J. Lin and C.-H. Lin are with the Department of Electrophysics, National Chiao Tung University, Hsinchu, Taiwan (e-mail: pillo.ep91g@nctu.edu.tw; lcs005.ep94g@nctu.edu.tw).

Y.-T. Li and C.-L. Pan are with Department of Photonics and the Institute of Electro-Optical Engineering, National Chiao Tung University, Hsinchu, Taiwan (e-mail: liyutai.ep91g@nctu.edu.tw; clpan@faculty.nctu.edu.tw).

R.-P. Pan is with the Department of Electrophysics, National Chiao Tung University, Hsinchu, Taiwan (e-mail: rpchao@mail.nctu.edu.tw).

Color versions of one or more of the figures in this letter are available online at <http://ieeexplore.ieee.org>.

Digital Object Identifier 10.1109/LPT.2009.2017382

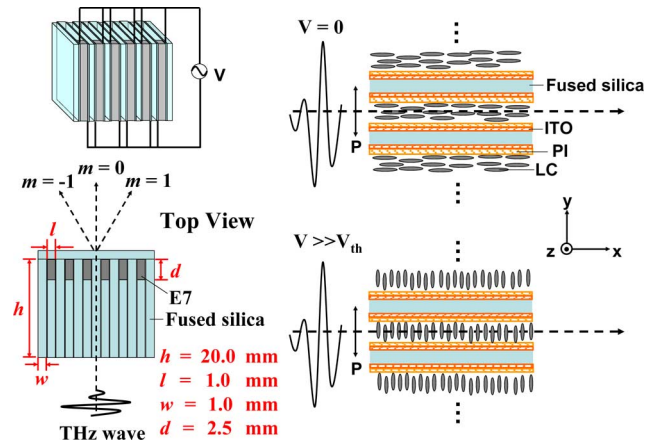


Fig. 1. Schematic drawing of the electrically controlled THz LC phase grating. The dimensions of the structure are shown. P: polarizer; PI: polyimide; V_{th} : threshold voltage.

field, E detected at an angle of ϕ from the incident beam can be written as

$$E_1(\phi) = \sum_{n=1}^{\text{odd}} \int_{nl}^{(n+1)l} E_0 e^{iky \sin \phi} e^{i(n_1 + i\kappa_1)kd} dy$$

$$E_2(\phi) = \sum_{n=0}^{\text{even}} \int_{nl}^{(n+1)l} E_0 e^{iky \sin \phi} e^{i(n_2 + i\kappa_2)kd} dy$$

and

$$E = E_1(\phi) + E_2(\phi) \quad (1)$$

where E_0 is the amplitude of the incident electric field, ϕ is the diffraction angle, k is the wave number of the electromagnetic wave in free space, l is the width of each material (assumed to be equal), d is the thickness of the grating, and $n_1 + i\kappa_1$ and $n_2 + i\kappa_2$ are complex refractive indices of materials 1 and 2, respectively.

Fig. 1 is a schematic drawing of the electrically controlled THz phase grating. The incident THz wave is polarized in the y -direction. Orientations of the LC molecules for two possible configurations are also shown. The device is designed such that the zeroth-order diffraction efficiency would be highest in the band around 0.3–0.5 THz. Parallel grooves having a period of 2.0 mm, a width of 1.0 mm, and a groove-depth of 2.5 mm are made by stacking indium tin oxide (ITO) coated fused silica plates with a refractive index of 1.95 in the sub-THz frequency region (0.2–0.8 THz). The fused silica surfaces are coated with polyimide (PI, SE-130B by Nissan), and then rubbed for homogenous alignment. The grooves are filled with a room temperature NLC (E7, Merck) and sealed with a fused silica plate

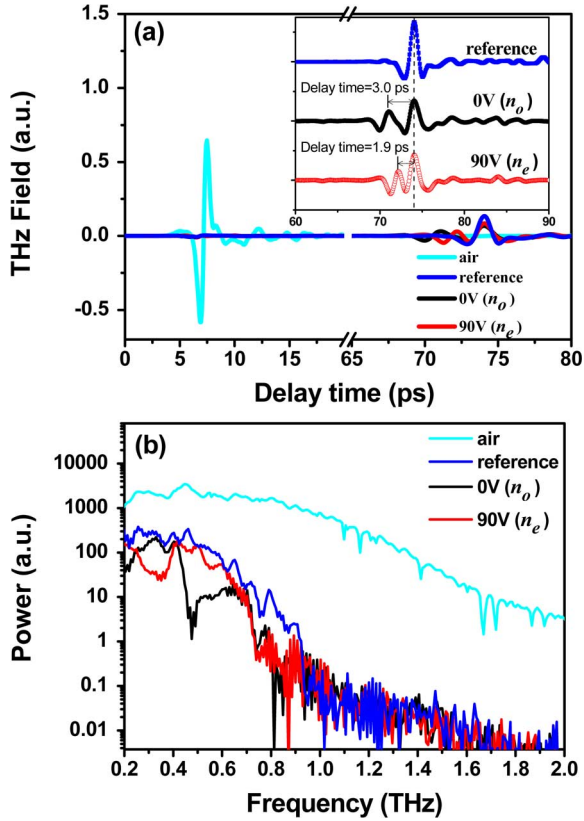


Fig. 2. (a) Time-domain and (b) spectral-domain characteristics of the device. Explanations of the various curves are given in the text.

coated with DMOAP (N, N- dimethyl-N-octadecyl-3-amino-propyltrimethoxysilyl chloride). Due to its positive dielectric anisotropy, the E7 molecules tend to be aligned parallel to the direction of the applied electric field when the applied voltage is larger than the threshold voltage. The effective refractive index of E7 [6], n_{eff} , can be tuned from the value for the ordinary wave ($n_o = 1.58$) to that for the extraordinary wave ($n_e = 1.71$) by varying the applied voltage.

The zeroth-order diffraction spectra of the device are detected with a photoconductive antenna-based THz time-domain spectrometer (THz-TDS) described previously [15]. A stack of ITO-coated fused silica plates identical in dimension to that of the grating is prepared as the reference for the THz-TDS. In the second set of experiments, the broadband THz signal is filtered by using a metallic hole array as a filter to yield a quasi-monochromatic wave centered at 0.3 THz with a line width of 0.03 THz [15]. The diffraction pattern of this beam by the grating with various NLC orientations is detected and mapped by a liquid-helium-cooled Si bolometer, 20 cm away from the device and located on a rotation arm that can be swung with respect to the fixed grating. The bolometer has an aperture about 2.5 cm in diameter.

III. RESULTS AND DISCUSSION

The zeroth-order diffracted THz pulses transmitted through the phase grating for both ordinary and extraordinary waves, (black and red curves), are shown in Fig. 2(a). For comparison, we also plotted the incident and the transmitted THz waveforms through the reference (the cyan and blue curves). The inset of

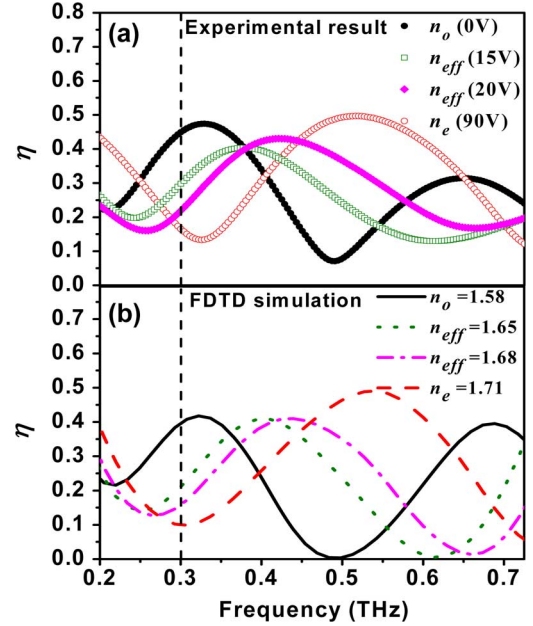


Fig. 3. (a) Experimental and (b) FDTD simulation results of the frequency dependence of the zeroth-order diffraction efficiencies of the phase grating operated at four applied voltages.

Fig. 2 shows a magnified view of the black, red, and blue curves. The spectral characteristics for all cases discussed in Fig. 2(a) are illustrated in Fig. 2(b).

The inset in Fig. 2(a) clearly shows oscillating components arriving 3.0 and 1.9 ps before the main pulse for ordinary and extraordinary waves, respectively. These are attributed to the propagation time difference between the waves through fused silica and NLC. The calculated times, $\delta nd/c$, where δn is the difference of the refractive indices between fused silica and NLC, d is groove depth and c is the speed of light in vacuum, are 3.1 and 2.0 ps, respectively. These are very close to the experimental observed time difference.

The diffraction efficiencies η in the frequency domain can be determined by normalizing the diffracted signals in the frequency domain with respect to that of the reference. Fig. 3(a) shows the experimentally determined diffraction efficiencies as a function of frequency with the device operating at 0, 15, 20, and 90 V. A finite-difference time-domain (FDTD) algorithm (RSoft Design Group, Inc.) is employed to simulate the diffraction of THz waves transmitted through the device. In the FDTD simulation, the size of the grid is $10 \mu\text{m} \times 10 \mu\text{m}$ while the time step is 1.67×10^{-14} s. The experimental and FDTD simulation results are in general agreement [see Fig. 3(b)]. There are, however, some discrepancies in efficiencies and peak positions. This is acceptable, as the thickness of the fused silica plates in the grating assembly varies by ± 0.1 mm. Further FDTD simulations show such variations could change efficiencies by 0.05 and the peak positions by 0.02 THz.

The experimental diffraction efficiency is highest near 0.3 THz, in agreement with the designed frequency. For ordinary wave at 0.3 THz, the phase difference between fused silica and E7 is close to 2π . Therefore, the transmission of the grating is higher. The THz wave is mainly concentrated in the zeroth order. In contrast, the phase difference is close to π for extraordinary waves. The diffraction efficiency is smaller for

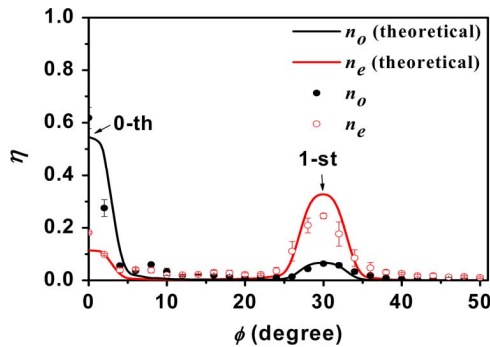


Fig. 4. Diffraction efficiency as a function of diffraction angle for the 0.3-THz beam.

the zeroth order, because the THz wave is mostly diffracted into the first order.

Fig. 4 illustrates the intensity profiles of the diffracted 0.3-THz-beam polarized in the y -direction. A diffraction maximum is detected at $\phi = 30^\circ$, which corresponds to the first-order diffracted beam that is predicted by the grating equation. The measured diffraction efficiencies for zeroth and first orders are also in good agreement with the theoretical values predicted by (1), taking into account the finite dimension of the grating and acceptance angle of the bolometer ($\pm 3^\circ$).

When the E7 molecules are aligned with n_{eff} equal to n_o , the phase difference is close to 2π . Most of the THz signal propagates in the direction of the zeroth-order diffraction. Experimentally, we find the diffraction efficiencies are 0.62 and 0.06 for the zeroth and first orders, respectively. On the other hand, when n_{eff} is equal to n_e , the phase difference is close to π . The THz wave propagates mostly as the first-order diffracted beam. The diffraction efficiencies are 0.18 and 0.25 for the zeroth and first orders, respectively. The grating would then function as a variable beam splitter. Varying the applied voltage, the beam splitting ratio of the zeroth to the first orders can be tuned from 10:1 to 1:1.

Overcoming the mechanical constraint of rotating the magnet without obstruction the THz wave in the previously reported magnetically tuned device [14], we are now able to vary the beam splitting ratio of the current device over a broader range. However, the transmittance of the electrically tuned phase grating is about half of the magnetically tuned one.

The stacked ITO-coated plates can be regarded as a waveguide that causes additional loss in transmittance. The energy of the incident THz pulse mainly distributed between 0.2 and 0.8 THz, much higher than the cutoff frequency of our device, 0.08 THz. According to the way we excited the waveguide and considering the resistive properties of the ITO layer, it was the TM mode traveling through the device. Following [16], the conductor losses are estimated to be 2.3 and 2.4 dB at 0.3 THz, for o-wave and e-wave, respectively, while the corresponding dielectric losses are 3.2 and 3.0 dB. The attenuation due to absorption and reflection at interfaces is about 1.5 dB. Thus the estimated total loss of the device is about 7 dB. Experimentally, the insertion loss of the grating for the zeroth-order diffracted wave at 0.3 THz is about 7–10 dB. The discrepancy could be due to finite collection efficiency of the detection system. By decreasing the thickness of fused silica plates in the base of the

device from 17.5 to 2.5 mm, the insertion loss can be reduced to 3–4 dB.

The periodic arranged ITO film can be considered as a wire-grid polarizer. Only the THz wave polarized perpendicular to the grooves can pass through the electrically tuned phase grating. The extinction ratio is 100:1 at 0.3 THz.

The turn-on and turn-off times of the grating are about 23 and 290 s, respectively. As a result, the present device is not suitable for applications that require fast modulation. Instead, the device is excellent for instrumentation or apparatus that require, e.g., a fixed beam splitting ratio with occasional fine tuning.

IV. CONCLUSION

We have demonstrated the feasibility of diffracting THz wave by an electrically controlled liquid crystal phase grating. The experimental results fit well with the FDTD calculation and theoretical prediction. This device can also be used as a beam splitter. The ratio of the zeroth- to first-order diffracted THz-beams (0.3 THz) polarized in a direction perpendicular to that of the grooves of the grating can be tuned from 10:1 to 1:1.

REFERENCES

- [1] P. Goldsmith, "Quasi-optical techniques," *Proc. IEEE*, vol. 80, no. 11, pp. 1729–1747, Nov. 1992.
- [2] M. Tonouchi, "Cutting-edge terahertz technology," *Nature Photon.*, vol. 1, pp. 97–105, 2007.
- [3] F. Garet, J.-L. Coutaz, M. Narzarov, E. Bonnet, O. Parriaux, and G. Racine, "THz time-domain spectroscopy study of grating couplers and segmented grating filters," in *Dig. Joint Int. Conf. Infrared Millimeter Waves and Terahertz Electron.*, 2004, pp. 181–182.
- [4] R. Kersting, G. Strasser, and K. Unterrainer, "Terahertz phase modulator," *Electron. Lett.*, vol. 36, pp. 1156–1158, Jun. 2000.
- [5] J. Chen, P. J. Bos, H. Vithana, and D. L. Johnson, "An electro-optically controlled liquid crystal diffraction grating," *Appl. Phys. Lett.*, vol. 67, pp. 2588–2590, 1995.
- [6] C.-Y. Chen, C.-F. Hsieh, Y.-F. Lin, R.-P. Pan, and C.-L. Pan, "Magnetically tunable room-temperature 2π liquid crystal terahertz phase shifter," *Opt. Express*, vol. 12, pp. 2625–2630, 2004.
- [7] H.-Y. Wu, C.-F. Hsieh, T.-T. Tang, R.-P. Pan, and C.-L. Pan, "Electrically tunable room-temperature 2π liquid crystal terahertz phase shifter," *IEEE Photon. Technol. Lett.*, vol. 18, no. 14, pp. 1488–1490, Jul. 15, 2006.
- [8] C.-Y. Chen, C.-F. Hsieh, Y.-F. Lin, C.-L. Pan, and R.-P. Pan, "Liquid-crystal-based terahertz tunable Lyot filter," *Appl. Phys. Lett.*, vol. 88, pp. 1–3, 2006, Article 101107.
- [9] I.-C. Ho, C.-L. Pan, C.-F. Hsieh, and R.-P. Pan, "A liquid-crystal-based terahertz tunable solc filter," *Opt. Lett.*, vol. 33, pp. 1401–1403, 2008.
- [10] C.-F. Hsieh, Y.-C. Lai, R.-P. Pan, and C.-L. Pan, "Polarizing terahertz waves with nematic liquid crystals," *Opt. Lett.*, vol. 33, no. 11, pp. 1174–1176, Jun. 1, 2008.
- [11] Z. Ghattan, T. Hasek, R. Wilk, M. Shahabadi, and M. Koch, "Sub-terahertz on-off switch based on a two-dimensional photonic crystal infiltrated by liquid crystals," *Opt. Commun.*, vol. 281, pp. 4623–4625, 2008.
- [12] S. Jewell, E. Hendry, T. Isaac, and J. Sambles, "Tunable Fabry–Perot etalon for terahertz radiation," *New J. Phys.*, vol. 10, pp. 1–6, 2008, Article 033012.
- [13] R.-P. Pan, C.-F. Hsieh, C.-Y. Chen, and C.-L. Pan, "Temperature-dependent optical constants and birefringence of nematic liquid crystal 5CB in the terahertz frequency range," *J. Appl. Phys.*, vol. 103, pp. 1–7, 2008, Article 093523.
- [14] C.-J. Lin, Y.-T. Li, C.-F. Hsieh, R.-P. Pan, and C.-L. Pan, "Manipulating terahertz wave by a magnetically tunable liquid crystal phase grating," *Opt. Express*, vol. 16, pp. 2995–3001, 2008.
- [15] C.-L. Pan, C.-F. Hsieh, R.-P. Pan, M. Tanaka, F. Miyamaru, M. Tani, and M. Hangyo, "Control of enhanced THz transmission through metallic hole arrays using nematic liquid crystal," *Opt. Express*, vol. 13, pp. 3921–3930, 2005.
- [16] D. K. Cheng, *Field and Wave Electromagnetics*, 1st ed. Reading, MA: Addison-Wesley, 1983, p. 465.